A Thesis Presented to

The Faculty of Alfred University

Sintering of Glass Bonded Silicon Carbide

by

Patrick G. Cigno

In Partial Fulfillment of
the Requirements for
The Alfred University Honors Program

5/12/2015

Under the Supervision of:

Chair: Dr. William Carty_____ _____
Committee Members:

Dr. David Lipke_____

Nik Ninos_____

Table of Contents

Page

List of Tables

Page

List of Figures

Page

Abstract

For applications where temperature is less than 1000°C, glass bonded SiC is an attractive option due to lower processing temperatures. To demonstrate this idea, clay was used to produce a glass phase during firing, resulting in amorphous grain boundaries on cooling. Results indicated that porosity was sensitive to clay concentration, but temperature had little effect. Samples containing 20% (by weight) clay had the lowest porosities (26-30%) and highest bulk densities; 5% (by weight) clay samples generated density levels averaging 58.50% of the theoretical, the lowest of all clay concentrations. Mullite and glass formation was temperature independent, which resulted constant skeletal density at all firing temperatures. These results offer the potential to tailor the porosity of sintered silicon carbide for less severe applications.

I. Introduction

Silicon carbide (SiC) is a material with many useful properties, including high oxidation resistance, very high hardness, heat resistance, and mechanical properties useful for many applications including high temperature applications. Silicon carbide's attractive properties (especially at high temperatures) are the result of the strongly covalent Si-C bond. However, this strong bond also makes silicon carbide difficult to sinter with high purity, requiring solid state sintering (and clean grain boundaries) and the use of expensive processes methods such as hot pressing that require high temperatures, pressures and an inert atmosphere to achieve high densities. However, these methods may be avoided with applications that don't require high density silicon carbide. Instead of solid state mechanisms, a bonding mechanism may be used to control porosity by wetting the grains, bonding the particles together, and filling in the structure instead of relying on extremely high firing temperatures to create a fully dense body. This study focuses on such a mechanism, using clay as a glass phase forming agent to control the open porosity in fired silicon carbide samples.

This study focuses on a temperature regime that will not create fully dense samples, but will allow the formation of a glass phase. Thus, high observed relative densities were not anticipated in this work, but the differences between the observed densities with varying levels of clay were important to consider. Significant changes in density would give insight to the effectiveness of the glass bonding mechanism in influencing the final porosity in the fired microstructure.

II. Experimental Procedure

A. Batching and Sample Preparation

In order to study the effect of the glass phase formed by clay, three different batches of SiC/clay were prepared with varying levels of clay content. Clay (EPK, Edgar Florida,) was added to SiC (400 Grit/ 22μm average) on a weight percent basis. Total batch mass prepared was 200[g]. The three weight percentages of clay used in this study were 5%, 12.5%, and 20% clay. To ensure the powders were well mixed, the prepared batches were jar milled for five minutes with alumina milling media on a ball mill. The compositions are listed in Table I below.

Table I. Prepared SiC/Clay Batches and Clay Composition

Batch	**Mass SiC**	**Mass Clay**	**Total Mass**
1	190.02[g]	10.01[g]	200.03[g]
2	175.01[g]	25.01[g]	200.02[g]
3	160.00[g]	39.98[g]	199.98[g]

Table II. Clay Composition.

Component	SiO_2	Al_2O_3	Na_2O	K_2O	MgO	CaO	Fe_2O_3	TiO_2
Wt.%	49.44	35.46	0.11	0.45	0.17	0.15	0.78	0.45

All samples used in this work were dry-pressed. The pressed pellets used a 19mm diameter die lubricated with oleic acid. A small amount of water was sprayed into the powder mix to improve final green pellet fidelity before pressing. No binder was added. All samples were pressed with a pressure of 78MPa. The pressed samples were left to dry in air at ambient temperatures for 24 hours before firing. Initial apparent volume measurements were taken by measuring the pellet dimensions.

B. Firing

Samples were fired to four different temperatures in order to observe any changes and/or development in microstructure. The temperature used in this study were 1200°C, 1300°C, 1400°C, and 1500°C. All samples were fired in ambient air; oxidation was not a concern in this work, although it could be considered in the future. Each firing run had a ramp rate of 5°C per minute, a dwell time at temperature of one (1) hour and a natural cool down. All runs contained nine (9) samples, three (3) from each batch described earlier. The furnace used in this study was a resistance (molybdenum disilicide heating element) vertical tube furnace. After firing, density measurements were calculated using an immersion method (ASTM C20 – 00^{1}) modified for small specimens. Apparent volume shrinkage was estimated by measuring pellet dimensions with calipers before and after firing.

C. Imaging

Selected samples for SEM imaging were broken to create a fracture surface, mounted, and sputter coated with AuPd. All of the prepared samples were viewed and imaged at different magnifications in order to compare the microstructures with varying clay content and firing temperatures.

III. Results and Discussion

A. Volumetric Shrinkage and Mass Loss

After firing, all the samples had surprising integrity. Apparent volumetric shrinkage was minor at all firing temperatures, reaching about 1%. Some samples even experienced an apparent volumetric expansion, again reaching about 1%. The lack of shrinkage indicates that little densification occurred, which is a topic that will be discussed later.

As firing temperatures increased, all concentrations of clay gradually lost less mass and even gained mass beginning at 1400°C. Changes in mass are summarized in Table II.

Table III. Change in Mass After Firing.

	Mass Change [g]			
	1200°C	**1300°C**	**1400°C**	**1500°C**
5% Clay	-0.67	+0.40	+1.94	+4.56
12.5% Clay	-1.00	-1.21	+0.20	+3.01
20% Clay	-0.84	-1.77	-1.42	+2.33

The mass loss can be explained by the dehydroxylation of the clay which occurs at 550°C.[2] With higher clay concentrations, there is more water, leading to more mass loss.

While EDX analysis was not conducted in this study, the gain in mass at higher temperatures indicates the formation of SiO_2 during firing. SiO_2 forms from passive oxidation reactions on the surface at lower firing temperatures near 1 bar of pressure.[3] The proposed reactions are as follows:

$$SiC(s) + 2O_2(g) \longrightarrow SiO_2(s) + CO_2(g) \quad (1)$$

$$SiC(s) + \tfrac{3}{2}O_2(g) \longrightarrow SiO_2 + CO(g) \quad (2)$$

Once a SiO_2 layer forms on the surface, oxidation is suppressed.[3] The formed SiO_2 also results in an increase in mass, demonstrated in Equation 1.

$$\frac{\Delta m}{m_0} = \frac{(60.09 g/mol) - (40.11 g/mol)}{(40.11 g/mol)} * 100 = 50\% \quad (3)$$

The mass gain from the conversion of SiC to SiO_2 with the clay dehydroxylation that stays constant relative to the amount of clay explains why the samples with more clay had lower mass gains; they lost more mass at the start from water, resulting in a lower net gain in mass at the end.

B. Density and Porosity

Fired densities were low across all clay concentrations. 20 weight percent clay had a higher average density at all firing temperatures and 5 weight percent had the lowest. 12.5 weight percent was in between but showed the most improvement with increasing firing temperature. However, the differences in apparent bulk density were not large and are summarized in Table III and plotted Figure 1 (utilizing standard error).

$$S.E \sqrt{\frac{\sum_{s=1}^{m} \sum_{i=1}^{n} y_{is}^2}{(n_y - 1)(n_y)}} \quad (4)$$

Where (*s*) is the series number, *(i)* is the point in series, (*m*) is the number of series for point *y* in the chart, (*n*) is the number of points in each series, (*yis*) is the data value of series (*s*) at the *i*th point, and (*ny*) is the total number of data values in all series.

Table IV. Average Apparent Bulk Density

Firing Temp. (°C)	**ρ [g/cm^3] 5% Clay**	**ρ [g/cm^3] 12.5% Clay**	**ρ [g/cm^3] 20% Clay**
1200	1.84	1.88	1.95
1500	1.91	2.02	2.02

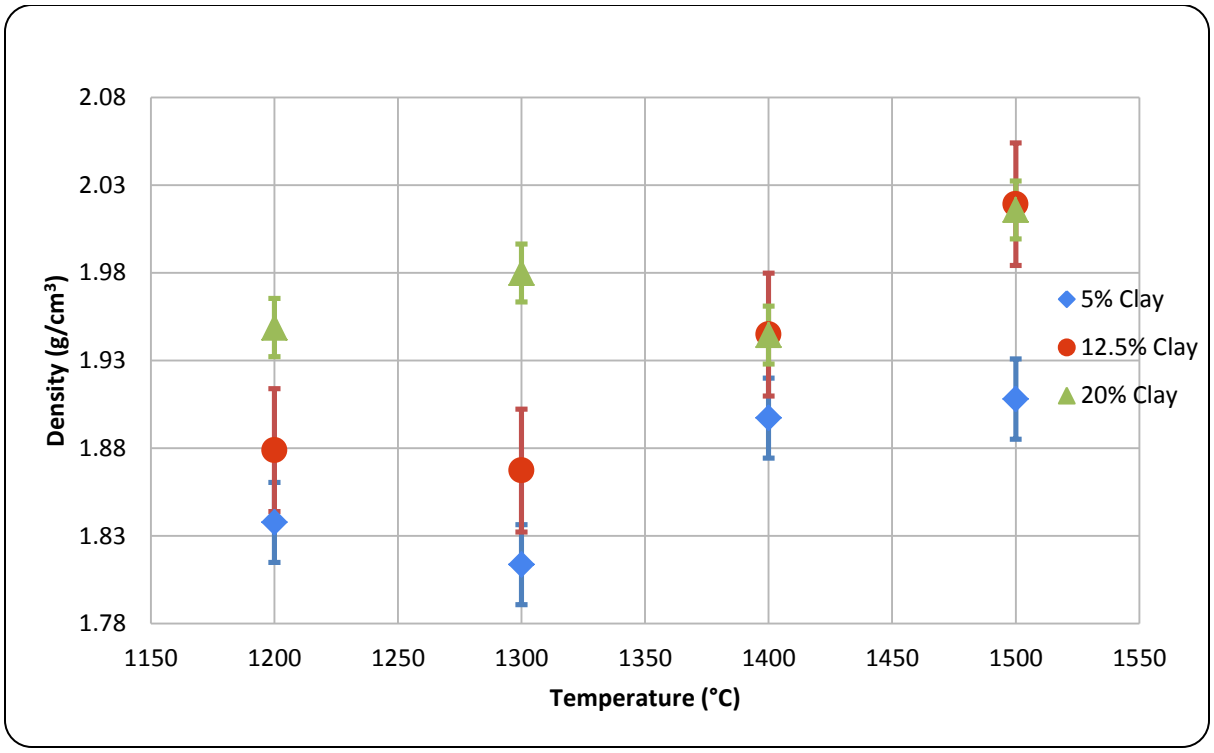

Figure 1. Average apparent bulk density of 5%, 12.5%, and 20% clay.

The same trend applied for the relative densities (compared to the calculated theoretical densities). 20% clay ranged from 65% to 67% theoretical density while 5% clay ranged from 57% to 60%. Again, 12.5% had the largest increase, ranging from 60.6% to 65.6%. Theoretical density was calculated using the Rule of Mixtures shown below.

$$\rho_{composite} = (f_{v,G} * \rho_G) + (f_{v,SiC} * \rho_{SiC}) + (f_{v,M} * \rho_M) + (f_{v,P} * \rho_P) \quad (3)$$

Where ρ is density and f is the volume percentage (summing to 1.0 or 100%) of the given component. The subscripts represent glass, SiC, mullite, and pores respectively. The calculated theoretical densities used an estimated glass phase density of 2.36 g/cm^3 (taking into account the effects of cristobalite) and a pore density of zero. The resulting theoretical densities are shown in Table IV.

Table V. Theoretical Densities of the SiC/Clay Samples

Wt.% Clay	**Vol. % Clay**	**Theoretical Density [g/cm^3]**
5.00	6.58	3.17
12.50	16.04	3.11
20.00	25.06	3.06

Porosity was essentially a mirror image of density, as expected. 5% clay had the greatest amount of porosity at all firing temperatures, 20% had the least, and 12.5% was in between, with the most reduction in porosity with increasing firing temperature. Porosity was calculated by dividing the internal open volume (obtained from the mass of water while determining bulk density through by immersion) by the apparent external volume, as seen in Equation 4.

$$f_{v,P} = \phi = \frac{V_{internal}}{V_{external}} * 100 \quad (4)$$

Where ϕ is porosity and V is volume, assuming no closed porosity. Porosity, like density, experienced little change with increasing firing temperature. 5% clay had porosities ranging from 37% to 31% while 20% clay ranged from 30% to 26% and 12.5% clay had the largest range, spanning from 37.7% to 26.3%. Additional clay content did reduce open porosity, though the change was not drastic. It is interesting to note that 12.5% clay behaved the most "traditionally," showing some improvement in densification and open porosity reduction with increasing firing temperature, while 5% and 20% did not improve as much with firing temperature. The average porosities are plotted in Figure 2.

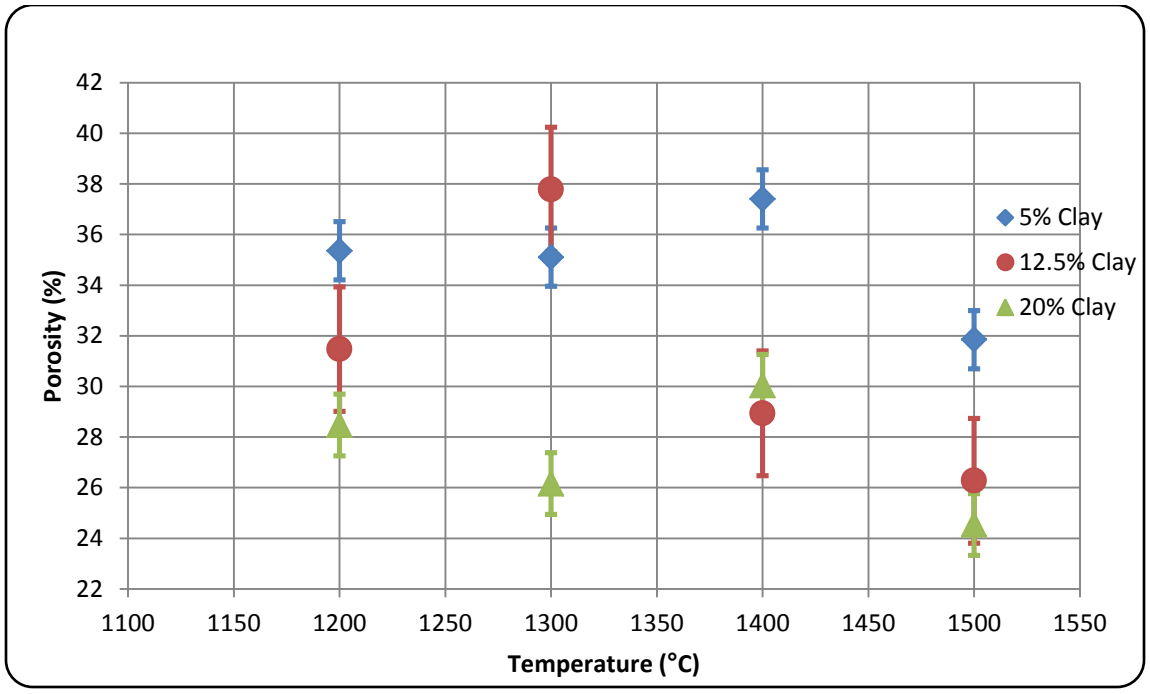

Figure 2. Average porosity of 5%, 12.5% and 20% clay.

Based off of the chemistry of the clay used in this work, some mullite formed during firing. Work by Tseng and Lerdprom[4-5] demonstrated that mullite can form at 1200°C, and thus will affect skeletal density. Not only was the amount of mullite formed small due to the limited amount of clay in the system, but it also remained constant with firing temperature, except for 20% clay samples, which showed a slight increase in both glass and mullite levels. 20% clay did form more mullite than 12.5% and 5%, but in all cases it was not enough to affect skeletal density. The estimated amount of glass and mullite formed is shown in Table V, assuming no free or amorphous quartz. The remaining clay remained amorphous or potentially formed cristobalite,[4] but due to limited amount of clay in the system, the amount is minimal, and could be incorporated into the effect of the glass.

Table VI. Glass and Mullite Level.

		Firing Temperature			
		1200°C	**1300°C**	**1400°C**	**1500°C**
5% Clay	Mullite [wt.%]	1.6	1.6	1.6	1.6
	Glass [wt.%]	2.9	2.9	2.9	2.9
12.5% Clay	Mullite [wt.%]	4.0	4.0	4.0	4.0
	Glass [wt.%]	7.3	7.2	7.2	7.2
20% Clay	Mullite [wt.%]	6.4	6.5	6.6	6.7
	Glass [wt.%]	11.5	11.7	11.8	12.1

The skeletal densities of the samples were comparable at all firing temperatures and clay concentrations, which helps reinforce the mullite formation data. Mullite has a density of 3.17g/cm^3, much greater than the 2.4g/cm^3 of the glass. Therefore, the more mullite formed, the higher the resulting skeletal density. The reason 20% clay samples had a similar skeletal density to 5% clay is because more glass was formed along with the additional mullite, canceling out the effect mullite would have had. The calculated skeletal densities are shown in Table VI.

Table VII. Skeletal Densities of the SiC/Clay Samples.

	Firing Temperature			
Wt. % Clay	**1200°C**	**1300°C**	**1400°C**	**1500°C**
5%	2.65 g/cm^3	2.70 g/cm^3	2.67 g/cm^3	2.64 g/cm^3
12.5%	2.60 g/cm^3	2.72 g/cm^3	2.54 g/cm^3	2.57 g/cm^3
20%	2.58 g/cm^3	2.67 g/cm^3	2.51 g/cm^3	2.55 g/cm^3

C. Microstructure

While different concentrations of clay did affect the resulting microstructure of the sample, there were some similarities. Glass formed at all temperatures but it was only marginally effective at bonding the structure together, even with 20% clay. No necking of the SiC grains occurred. 1500°C was not hot enough, or the hold time at temperature

was not long enough. The system relied entirely on the glass bonding the SiC grains together. Figure 3 highlights the microstructures.

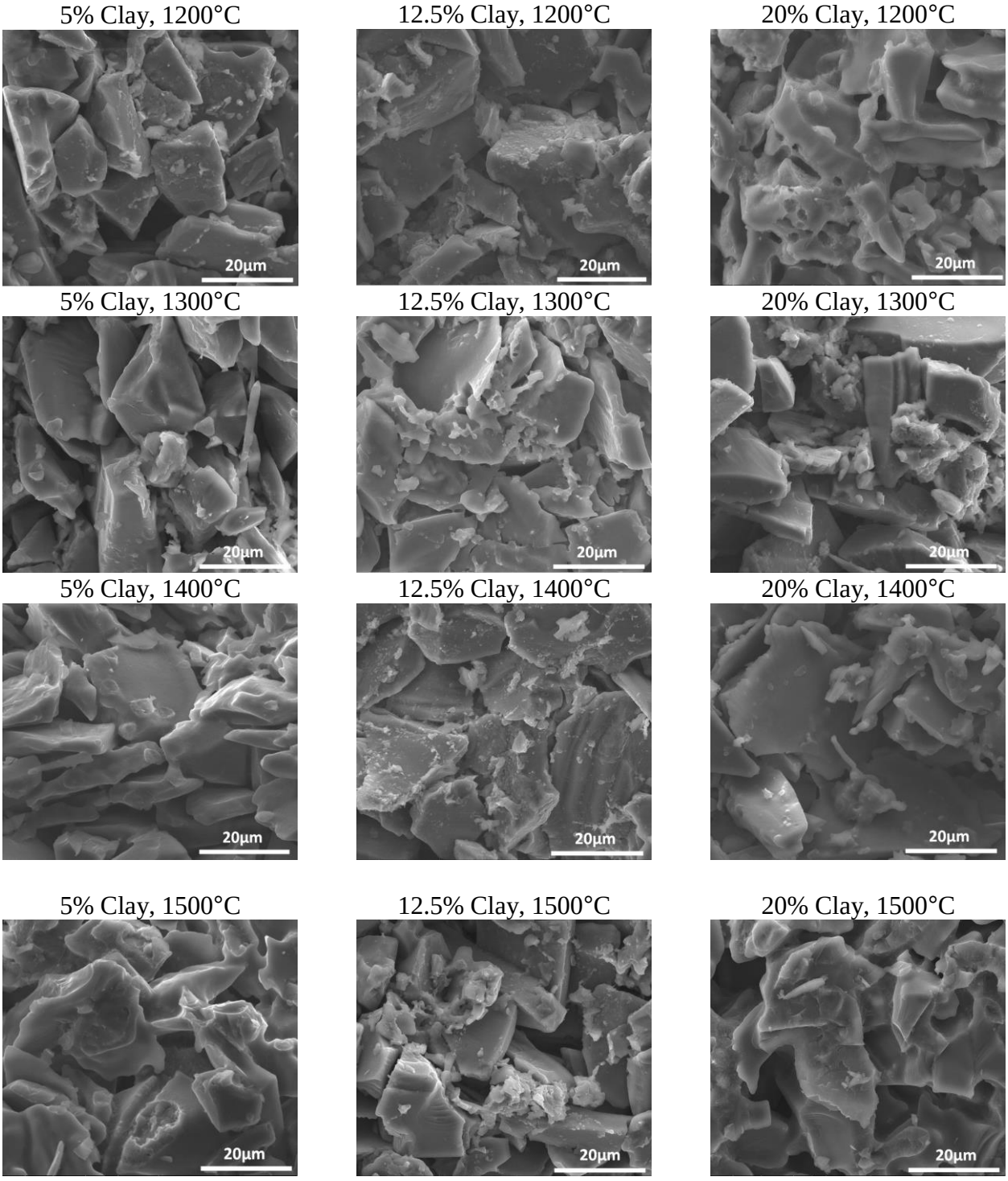

Figure 3. Microstructures of 5% (left), 12.5% (middle), and 20% (right) clay.

Firing temperature had little effect on the resulting microstructure. While the glass did aid in the formation of amorphous grain boundaries, the structures still had similar porosities with varying clay content. 5% and 12.5% clay fired at 1200°C still contained well defined grains and boundaries, which slightly improved with increasing temperature. While 20% clay had more amorphous boundaries at 1200°C from having additional glass, the amount of glass formed remained constant. Therefore the microstructure at 1500°C still closely resembles the one after firing at 1200°C. The SiC grains showed essentially zero activity in this temperature range. The addition of clay did not catalyze necking behavior between grains. Since no necking occurred, neither did grain growth since grain growth occurs after necking. This is supported by relative stability in the amount of porosity observed in the samples and the minor increases in bulk density.

Bonded SiC systems provide some advantages. Firing temperatures to reach desired densification levels are lower and linear shrinkage can be near-zero. Mullite based systems can take advantage of SiO_2 formed from oxidation by growing mullite needles in situ with Al_2O_3 either with pure alumina or with bauxite above 1400°C, and longer hold times at temperature can result in particle necking.[6-8] Bonding can also be achieved without Al_2O_3, relying on the formation of cristobalite between grains from amorphous SiO_2, though doing so results in higher porosity.[9] Bonded SiC bodies also provide the opportunity to tailor porosity though the addition of carbon. Graphite oxidation begins at approximately 600°C, forming gaseous CO_2 or CO. Changing the amount of graphite as well as the graphite particle size changes the amount of open porosity and the pore size distribution as the gaseous oxidation products leave the

system.[7-9] The results from these studies indicate that mullite not only increases skeletal density, but also plays a role in bonding the SiC grains together. The similar density and thermal expansion coefficient of mullite to SiC also improves the mechanical properties of the resulting porous composite. This makes clay more promising as it does form mullite, but not nearly as much as other systems that used an oxidation bonding approach.

Lim showed a similar effect with starch content in a sodium-borate bonded system, and found that increasing the firing temperature while keeping starch concentration (the pore former) constant reduced porosity by partial pore filling due viscous flow of the sodium borate. Porosity can also be controlled in glass bonded systems through particle size and concentration.[10] Wang found that increasing SiC concentration reduces porosity when a 61% (by weight) SiO_2, 24% Al_2O_3, 5% CaO, 2% Na_2O, 2% K_2O, and 6% other materials glass forming system was used.[11] Porosity increased from 32.1% porosity at 65 volume percent SiC to 64.7% at 85 volume percent when fired at 850°C for 1 hour. The data collected here showed similar results; higher SiC content (lower weight percent clay) resulted in higher porosity. The study also demonstrated that decreasing SiC particle size increased porosity due to increased surface area, but the average pore size was reduced, but this claim can't be supported or refuted by this work; only one particle size was used. Most of these studies used concentrations of pore, mullite, or glass forming phases that exceed 20 weight percent, which indicates that better results may be obtained with a higher clay concentration (more mullite and glass would form and may improve the bonding of the SiC grains).

It is unclear how effective clay would be as a sintering aid at higher temperatures. Work on SiC reactivity by Negita indicated that Al_2O_3 is an effective sintering aid for SiC

at high temperatures (2000°C), but CaO, MgO, TiO_2, and Fe_2O_3 (all impurities found in the clay used in this work) are not.[12] The formed glass phase may also dissolve SiC in order to scavenge additional SiO_2 as well, which could affect grain growth at higher temperatures.

IV. Conclusion

Porosity in the SiC/Clay composite was sensitive to clay concentration, but temperature had essentially no effect. A higher firing temperature which allows necking and/or grain growth to occur in the SiC grains may show temperature dependence, but lower firing temperatures shows no dependence. 20% clay led to the highest bulk density and lowest porosity at all firing temperatures, and 5% clay led to the most porosity and lowest bulk density, averaging at 58% of the calculated theoretical density. Glass and mullite formation remained constant with firing temperature; higher clay concentrations resulted in more glass and mullite.

These results offer the potential to control the porosity of sintered SiC. Varying the amount of glass phase formed can change the open porosity in a SiC composite, even at very low firing temperatures. While these composites are not suitable for extreme conditions, they could be useful in other applications such as construction materials or similar applications that do not require high purity. This method of porosity control could potentially lower processing costs, depending on the firing temperature and glass phase used in the composite.

V. Bibliography

1. "Standard Test Methods for Apparent Porosity, Water Absorption, Apparent Specific Gravity, and Bulk Density of Burned Refractory Brick and Shapes by Boiling Water" ASTM Designation C20-00. American Society for Testing and Materials, West Conshohocken, PA.

2. V. Colorado, *Fast Firing of Porcelain*, M.S. Thesis, Alfred University, Alfred NY, 2014.

3. J. Roy, S. Chandra, S. Das, and S. Maitra, "Oxidation Behaviour of Silicon Carbide- A Review," *Rev. Adv. Mat. Sci.,* **38** [1] 29-39 (2014).

4. K. Tseng, H. Lee, and W. Carty, "A Potential Short-Cut to Quantitative Mineralogy." *Proceedings of the 51st Annual Symposium on Refractories St. Louis Section of the Am. Ceram. Soc.,* St. Louis, MO, (2015).

5. W. Lerdprom, *Firing of Porcelain*, M.S Thesis, Alfred University, Alfred NY, 2014.

6. K. Changming, J. Edrees, and A. Hendry, "Fabrication and Microstructure of Sialon-bonded Silicon Carbide," *J. Eur. Ceram. Soc.,* **19** [12] 2165-2172 (1999).

7. S. Ding, S. Zhu, Y. Zeng, and D. Jiang, "Fabrication of Mullite-bonded Porous Silicon Carbide Ceramics by *In Situ* Reaction Bonding," *J. Eur. Ceram. Soc.,* **27** [4] 2095-2102 (2007).

8. C. Bai, Y. Li, Z. Liu, P. Liu, X. Deng, J. Li, and J. Yang, "Fabrication and Properties Mullite-bonded porous SiC Membrane Supports Using Bauxite as Aluminum Source," *Ceram. Int.,* **41** [3] 4391-4400 (2015).

9. J. She, Z. Deng, J. Daniel-Doni, and T. Ohji, "Oxidation Bonding of Porous Silicon Carbide Ceramics," *J. Mater. Sci.,* **37** [17] 3615-3622 (2002).

10. K. Lim, Y. Kim, and I. Song, "Porous Sodium Borate-bonded SiC Ceramics," *Ceram. Int.,* **39** [6] 6827-6834 (2013).

11. B. Wang, H. Zhang, H. Phuong, F. Jin, J. Yang, and K. Ishizaki, “Gas Permeability and Adsorbability of the Glass-bonded Porous Silicon Carbide Ceramics with Controlled Pore Size,” *Ceram. Int.,* **41** [2A] 2279-2285 (2015).

12. K. Negita, “Effective Sintering Aids for Silicon Carbide Ceramics: Reactivities of Silicon Carbide with Various Additives,” *J. Am. Ceram. Soc.,* **69** [12] 308-310 (1986).